AD_____

Award Number: W81XWH-07-1-0218

TITLE: Non-Invasive Nanodiagnostics of Cancer (NINOC)

PRINCIPAL INVESTIGATOR: Alexander Kabanov, Ph.D.

CONTRACTING ORGANIZATION: University of Nebraska Medical Center
Omaha, NE 68198-7835

REPORT DATE: April 2008

TYPE OF REPORT: Annual

PREPARED FOR: U.S. Army Medical Research and Materiel Command
Fort Detrick, Maryland 21702-5012

REPORT DOCUMENTATION PAGE

Form Approved
OMB No. 0704-0188

1. REPORT DATE	2. REPORT TYPE	3. DATES COVERED
01-04-2008	Annual	1 Apr 2007 - 31 Mar 2008

4. TITLE AND SUBTITLE

Non-Invasive Nanodiagnostics of Cancer (NINOC)

5a. CONTRACT NUMBER

5b. GRANT NUMBER
W81XWH-07-1-0218

5c. PROGRAM ELEMENT NUMBER

6. AUTHOR(S)

Alexander Kabanov, Ph.D.

E-Mail: akabanov@unmc.edu

5d. PROJECT NUMBER

5e. TASK NUMBER

5f. WORK UNIT NUMBER

7. PERFORMING ORGANIZATION NAME(S) AND ADDRESS(ES)

University of Nebraska Medical Center
Omaha, NE 68198-7835

8. PERFORMING ORGANIZATION REPORT NUMBER

9. SPONSORING / MONITORING AGENCY NAME(S) AND ADDRESS(ES)
U.S. Army Medical Research and Materiel Command
Fort Detrick, Maryland 21702-5012

10. SPONSOR/MONITOR'S ACRONYM(S)

11. SPONSOR/MONITOR'S REPORT NUMBER(S)

12. DISTRIBUTION / AVAILABILITY STATEMENT
Approved for Public Release; Distribution Unlimited

13. SUPPLEMENTARY NOTES

14. ABSTRACT

This project seeks to develop noninvasive diagnostics to detect cancer in its earliest, most easily treatable, pre-symptomatic stage. Innovative imaging nanomaterials and delivery technologies is employed to target, label and detect the cancer cells within the body at sites which are normally inaccessible to conventional diagnostic methods. The hydrophilic polymer nanogels of core-shell morphology are designed to entrap different types of probes used in single photon emission computed tomography, computer tomography, magnetic resonance or luminescence detection. The surface of the nanogels is modified with genetically engineered antibody fragments to target the surface of cancer cells and provide site-specific delivery of the nanogels to tumors in the body.

15. SUBJECT TERMS
noninvasive diagnostics to detect cancer

16. SECURITY CLASSIFICATION OF:			17. LIMITATION OF ABSTRACT	18. NUMBER OF PAGES	19a. NAME OF RESPONSIBLE PERSON
a. REPORT	b. ABSTRACT	c. THIS PAGE			19b. TELEPHONE NUMBER *(include area code)*
U	U	U	UU	24	USAMRMC

Standard Form 298 (Rev. 8-98)
Prescribed by ANSI Std. Z39.18

Table of Contents

Page

INTRODUCTION

One of the most reliable predictors of cancer survival is tumor size at the time of diagnosis; therefore it is important to identify cancerous tumors as early as possible. Currently available technologies are powerful for the detection of large tumors with specificity; however, smaller tumors are difficult to detection due to the lack of sensitivity. This project seeks to develop noninvasive diagnostics that combine the specificity of tumor associated antigen expression in cancer with imaging probe of nanoscale size with the objective to advance our capacity for identification and characterization of the malignancy in its initial, most easily treatable stages. *The overall objective is to develop a better diagnostic strategy for noninvasive imaging of colon cancer by using novel targeted cross-linked nanogels of nanoscale size as contrast-enhancing probes*. It is anticipated that the development of this testing methodology and nanoprobe technology will be broadly applicable to cell specific contrast agents in other cells with specific molecules or receptors that can be targeted by antibodies or molecules attached to the nanoprobe surface. Novel type of functional nanomaterials- nanogels of core-shell morphology – is utilized as a platform for design of imaging probes. These nanogels represent hydrophilic nanospheres, which combine several key structural features: a cross-linked ionic core; a hydrophilic protective shell; and nanoscale size. Contrast reporter moieties can be efficiently incorporated into multifunctional ionic core of the nanogels. The end groups in the shell of the nanogel may be modified with vector ligands for active targeting, leading to multivalent recognition of probe targets. Targeted delivery of the polymer carrier to a mucin overexpressed on most colon carcinoma cells, such as TAG72 antigen, would enhance the selectivity of noninvasive imaging when used in this context. Since the delivery and detection principles are universal, the same nanocarriers can be used with different contrast reporter moieties such as inexpensive and short-lived radioisotopes, Gd(III)-chelates, or fluorescent probes which allows multiple methods of detection based on different physical principles, such as single photon emission computed tomography (SPECT), magnetic resonance (MR) or optical detection.

BODY OF REPORT

This section describes the efforts devoted by the program team to meet the major technical objectives that were: 1) set up of the project; 2) synthesis and characterization of nanogels with cross-linked ionic cores from poly(carboxylic acid) chains and a hydrophilic shell from poly(ethylene oxide) (PEO) chains, 3) select the antibodies to a tumor epitope ; 4) develop the procedures for conjugation of antibodies to nanogels; 5) incorporate MR and optical probes in nanogels; and 6) *in vivo* "proof of concept" studies using an animal tumor model to evaluate the degree to which the designed imaging probes have the potential to provide detection of colon cancer cells.

Task 1 -- Set up project

The major goal of this task was to assemble an interdisciplinary team of the scientists involving leading experts from cancer research, pharmacy, and medicine as well as professional staff to conduct the proposed studies. The research team was assembled under the leadership of Dr. Alexander Kabanov, Parke-Davis Professor of Pharmaceutical Sciences and Director of the Center for Drug Delivery and Nanomedicine, College of Pharmacy at University of Nebraska Medical Center. The senior investigators participated in the research project are: Dr. Surinder Batra, Professor in the Department of Biochemistry and Molecular Biology, an expert in area of cancer biology with longstanding interests on mucins, specifically in biology of the mucin-type glycoprotein MUC4 in cancer; Dr. Michael Boska, Professor and Vice Chairman of Research at the Department of Radiology, with an extensive expertise in the development of quantitative MRI technologies; Dr. Tatiana Bronich, Associate Professor of Pharmaceutical Sciences and Associate Director of the Center for Drug Delivery and Nanomedicine, an accomplished polymer chemist with extensive experience in the areas of material science and nanoscale assembly, including the nanofabrication of nanogels; Dr. Serguei Vinogradov, Research Associate Professor at the Department of Pharmaceutical Sciences, an expert in organic chemistry of biologically active compounds and chemical engineering of biological macromolecules; Dr. Maneesh Jain, Assistant Professor in the Department of Biochemistry and Molecular Biology, experienced in development of genetically engineered antibody fragments for improved radioimmunotherapy of solid tumors. Dr. R. Lee Mosley, Assistant Professor in the Department of Pharmacology and Experimental Neuroscience, is an expert in non-invasive small animal SPECT imaging and will supervise these studies in the research project. Dr. Janina Baranowska-

Kortylewicz, Professor in the Department of Radiation Oncology, radiochemist and expert in the areas of imaging agents, radioimmunotherapeutics, and radiolabeled nucleic acid precursors for cancer therapy. Dr. Kortylewicz has been active in the development of pro-drugs designed to provide more effective systemic radiotherapy for a variety of malignancies and is serving as a consultant on this project. She was invited to serve as a consultant on the project.

Imaging operator, Nan Gong,M.D., was hired for this program specifically to conduct all image acquisitions and data analysis. She is working close with Dr. Boska and Dr. Lee and is responsible for performing SPECT studies. A chemist, Mrs. Nataliya Nukolova, who has M.S. degree in organic chemistry, was involved in the all steps of the synthesis and modification of the nanogls.

Organizational meeting of the team discussed and finalized a work plan and identify the current and long-term goals of each task.

During the first year of the program the following equipment for the characterization of nanoparticulates was acquired: ACTA FPLC system (GE Healthcare Biosciences Group) for fast and easy purification of proteins and other macromolecules; differential refractometer, Smartline RI detector 2300 (Knauer), was assembled with ACTA FPLC system for detecting compounds without UV activity; HPLC system (Agilent 1200 Series LC, Agilent Technologies) equipped with quaternary pump with degasser, autosampler, diode array and fluorescent detectors, and temperature controller. Agilent HPLC system was connected to Model 302 Tetra Detector Platform from Viscotek, multiple-detector device that combines low angle light scattering with UV, viscometry, and refrective index measurements and operates on-line in continuous-flow mode. BI-200SM Research Goniometer (Brookhaven Instruments Corp.) and differential refractometer operated at the same wavelength as the goniometer (determines differential refractive index increment, *dn/dc*); Zetasizer Nano ZS (Malvern); SpectraMax 5M multi-detection microplate reader (Molecular Devices). Fluorolog-3 research spectrofluorometer (Horiba Jobin Yvon) has been ordered.

Protocol of the animal research entitled “Non-invasive Nanodiagnostics of Cancer (NINOC)” was prepared and approved to UNMC Institutional Animal Care and Use Committee (IACUC) on 08/06/2007 (protocol # 07-041-07-FC). The animal protocol was further submitted and approved by USAMRMC Animal Care and Use Review Office (ACURO) (09/12/2007).

Task 2 -- Synthesize and characterize nanogels

Block ionomers represent block (or graft) copolymers containing ionic and nonionic polymeric segments. Such block copolymers react with oppositely charged species forming block ionomer complexes, which self-assemble into core-shell micelles of nanoscale size. Diblock copolymers containing anionic and nonionic hydrophilic polymeric segments were used to prepare polyion complex micelles, templates for the synthesis of nanogels. Polymethacrylic acid (PMA) and polyacrylic acid (PAA) were used as anionic blocks. Poly(ethylene oxide), PEO, was used as a hydrophilic block. PEO-b-PMA and PEO-b-PAA with various length of anionic and PEO segments were purchased from Polymer Source Inc. (Montreal, Canada). The characteristics of block copolymers used in these studies are summarized in ***Table 1***. Diblock copolymer samples are denoted as PEO(*x*)-*b*-PMA(*y*) or PEO(*x*)-b-PAA(*y*), where *x* and *y* represent the degree of polymerization of the PEO segment and PMA or PAA segment, respectively.

Table 1. Physico-chemical characteristics of block copolymers

Block copolymer[a]		Molecular weight	Polydispersity index
PEO 7500-*b*-PMA 15500	PEO(170)-*b*-PMA(180)	23,000	1.45
PEO 5500-*b*-PMA 15500	PEO(125)-*b*-PMA(180)	21,000	1.16
PEO 5000-*b*-PMA 7000	PEO(114)-*b*-PMA(81)	12,000	1.15
PEO 3500-*b*-PAA 7500	PEO(80)-*b*-PAA(104)	11,000	1.25
PEO 5000-*b*-PAA 6700	PEO(114)-*b*-PAA(93)	11,700	1.20

[a]The average number of ethylene oxide and carboxylic acid units (in parentheses) in block copolymers were calculated using the average molecular weights provided by manufacturer

The synthesis of nanogels was carried out as outlined in ***Figure 1.*** The first step involved self-assembly of PEO-*b*-PMA(or PAA) copolymers into polymer micelles in the presence of divalent cations such as Ca^{2+} or Ba^{2+}. Electrostatic neutralization of polyion block by metal ions induces amphiphilicity and results in spontaneous

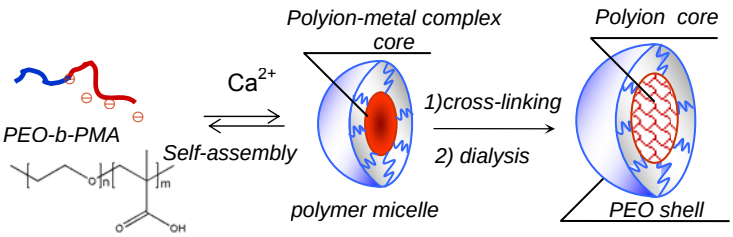

Figure 1. Scheme for the synthesis of nanogels with cross-linked ionic cores

micellization of the copolymer. The sizes of the PEO(*x*)-*b*-PMA(*y*) /Ca^{2+} micelles were determined by dynamic light scattering and are presented in Table 2. The low polydispersity indices (<0.1) suggested a narrow particle size distribution of the prepared PEO(170)-b-PMA(180) /Ca^{2+} and PEO(125)-b-PMA(180) /Ca^{2+} micelles. The samples exhibited no particle size changes while standing at room temperature for at least several days. The complex formation was completely abolished by adding an equimolar amount of a Ca^{2+} chelating agent, ethylenediaminetetraacetic acid (EDTA) into the reaction mixture.

Table 2. Effective diameters of PEO(*x*)-*b*-PMA(*y*) /Ca^{2+} complexes

Copolymer	PEO(170)-*b*-PMA(180)	PEO(125)-*b*-PMA(180)	PEO(114)-*b*-PMA(81)
D_{eff}[a], nm	90	100	n/a

[a] Effectiive diameter denote averaged value calculated from three measurements performed on each sample. D_{eff} values were within ± 5 nm.

Notably, in the case of PEO(114)-b-PMA(80) copolymer no complex formation was detected in the presence of Ca^{2+} ions. However, the onset of the self-assembly and turbidity increase were observed in PEO(114)-b-PMA(80) /Ba^{2+} mixtures at a relatively large excess of Ba^{2+} ions. The block ionomer-metal complexes can be considered as a special type of the copolymer with neutralized, water-insoluble segments from the polyion-metal complex and water-soluble PEO chains. The relative ratio of neutralized and polyether segments determined the solution properties of the complexes. The presence of higher content of hydrophilic PEO segments in the PEO(114)-*b*-PMA(81) copolymer provided for additional hydrophilicity of the corona-forming chains and affected the onset of self-assembly in the PEO(114)-*b*-PMA(81) /Me^{n+} mixtures which is shifted towards higher concentration of condensing agent.

At the second step, the inner core of the micelles formed was cross-linked through the carboxylic groups using bifunctional agent, 1,2-ethylenediamine, in the presence of 1-(3-dimethylaminopropyl)-3-ethylcarbodiimide hydrochloride (EDC). The byproducts of the cross-linking reaction and metal ions were removed by exhaustive dialysis of the reaction mixtures, against (1) 0.5% aqueous ammonia in the presence of EDTA, and (2) distilled water. The particles with the net negative charge and diameters in the range of 140 – 215 nm were present in the aqueous dispersions (***Table 4***). It is important to note that the sizes of the formed cross-linked nanogels were significantly larger than the sizes of the original copolymer/Me^{n+} micellar templates. For example, cross-linked PEO(170)-*b*-PMA(180) nanogels of hydrodynamic diameters

of ca. 215 nm were produced from the PEO(170)-*b*-PMA(180)/Ca^{2+} micelles of 90 nm in diameter. This corresponded to the 2.4-fold increase in the diameter and 14-fold increase in the volume of the particles. Such an expansion was consistent with the removal of metal ions and formation of water-swollen nanostructures.

Table 3. Physicochemical characteristics of nanogels with cross-linked ionic core at pH 7.0.

Copolymer	Template composition	D_{eff}[a], nm	ζ,[b] mV
*cl*PEO(170)-*b*-PMA(180)	$[Ca^{2+}]/[COO]=1.3$	157	-21
*cl*PEO(125)-*b*-PMA(180)	$[Ca^{2+}]/[COO]=0.8$	176	-25
*cl*PEO(114)-*b*-PMA(81)	$[Gd^{3+}]/[COO]=0.4$	141	-23
*cl*PEO(114)-*b*-PAA(93)	$[Ba^{2+}]/[COO]=1.6$	169	-32

[a] Effectiive diameter denote averaged value calculated from three measurements performed on each sample. D_{eff} values were within ± 5 nm.

[b] ζ - potential values were calculated from three measurements performed on each sample and were within ± 5 mV.

These data demonstrated that the physicochemical properties of the nanogels are strongly dependent on structure of diblock copolymer.

Since the swelling properties of hydrogels strongly depend on polymer cross-linking degree, the structure of the cross-linker and the number of cross-links will dictate the composition and properties of the nanogel cross-linked cores and, thus, directly control the swelling behavior of the nanogels. To elucidate the effects of the cross-linking density of the core upon the properties of the micelles, the cross-linked micelles were prepared from the same stock solution of template PEO(170)-b-PMA(180)/Ca^{2+} micelles with targeted degree of cross-linking from 10% to 60%. The targeted percentage of cross-linking was based on the ratio of amine functional groups to carboxylic acid groups. The extent of targeted cross-linking represents the maximum theoretical amount of cross-linking that can take place, rather than the precise extent of amidation, which is expected to be lower. Indeed, the efficiency of the carbodiimide-induced cross-linking reaction is affected strongly by a side reaction between water and the activated carboxylic groups that competes with the condensation reaction. In addition, the diamine could react either with two separate PMA chain segments to yield a cross-link or to form a “loop” being bound to the same PMA chain as well as attach by only one amino group giving the free amine. Due colloidal nature of the nanogels conventional solution-state ^1H NMR allowed us only to estimate the changes in the extent of cross-linking upon the synthesis (***Figure***

2). As expected, the number of cross-links introduced into the core of the micelles increased with the increase of targeted degree of cross-linking. Those having a lower degree of cross-linking (i.e. 10% and 20%) underwent more extensive swelling upon increase of pH whereas a modest increase in the D_{eff} was observed for the nanogels with the targeted degree of swelling of 40% and higher (***Figure 3***).

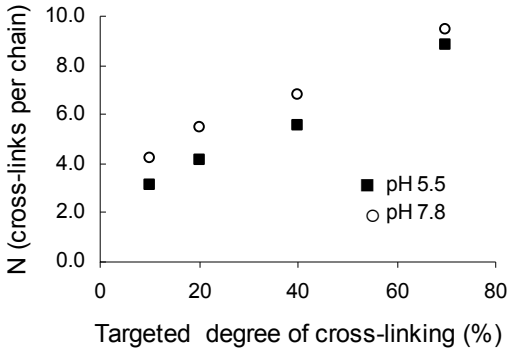

Figure 2. Relative number of cross-links per chain in PEO(170)-*b*-PMA(180) nanogels as a function of targeted degree of cross-linking.

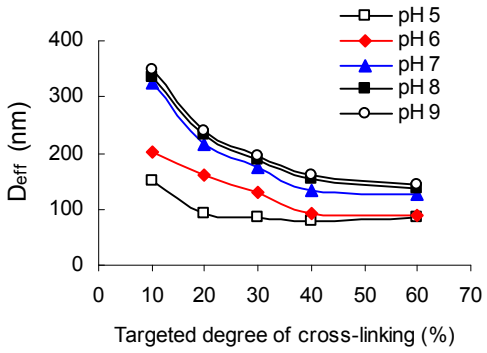

Figure 3. Effective diameter (D_{eff}) of cross-linked PEO(170)-*b*-PMA(180) nanogels at various pH as a function of targeted degree of cross-linking.

Further, we explored the effects of the hydrophobicity and the length of cross-linker on the structure and swelling properties of the PEO(170)-b-PMA(180) nanogels using several diamino cross-linkers. 1,2-ethylenediamine, 1,5-diaminopentane, cystamine HCl, and 2,2'-(ethylenedioxy)bis (ethylamine) were used to cross-link the cores of template PEO(170)-b-PMA(180)/Ca^{2+} micelles with targeted degree of cross-linking up to 60%. It was anticipated that the relatively hydrophobic core of the PEO-*b*-PMA /Ca^{2+} micelles would impose some restrictions for the permeability of rather hydrophilic cross-linkers such as ethylenediamine or 2,2'-(ethylenedioxy)bis (ethylamine), and might be favorable for the more hydrophobic cross-linkers. The incorporation of more hydrophobic cross-linkers into the core of the micelles also resulted in the formation of nanogels with smaller sizes (***Figure 4***). As expected, the number of cross-links in the nanogels was elevated when more hydrophobic cross-liker was used (***Figure 5***). As a result the swelling of the core of such nanogels upon increase of pH was suppressed: only a modest increase in the D_{eff} was observed for the micelles with hydrophobic cross-linkers (e.g. 1,5-diaminopentane) (***Figure 4***).

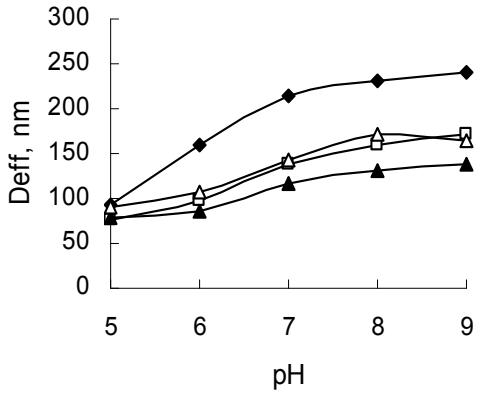

Figure 4. Effective diameter (D_{eff}) of cross-linked PEO(170)-*b*-PMA(180) nanogels at various pH: :(✦) ethylenediamine; (☐)1,5-diaminopentane; (▲) cystamine; (∆)2,2' (ethylenedioxy) bis (ethylamine).

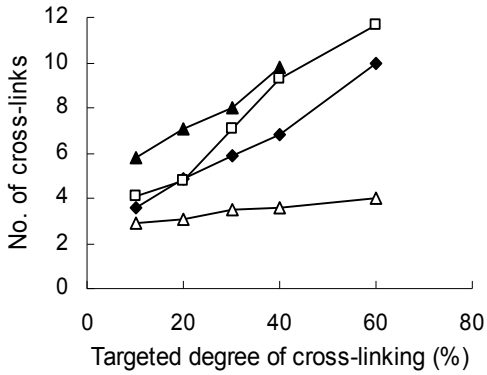

Figure 5. Relative number of cross-links per chain in PEO(170)-*b*-PMA(180) nanogels as a function of targeted degree of cross-linking:(✦) ethylenediamine; (☐)1,5-diaminopentane; (▲) cystamine; (∆)2,2' (ethylenedioxy) bis (ethylamine).

Diblock copolymer PEO(125)-*b*-PMA(180) was synthesized by anionic polymerization of tert-butylmethacrylate first followed by ethylene oxide and its hydrolysis (information was provided by manufacturer, Polymer Source Inc.). As a result the hydroxyl group was an end group in the PEO chains of this copolymer. This copolymer sample was further used to synthesize nanogels with cross-linked cores and reactive terminal groups in PEO corona. PEO(125)-*b*-PMA(180) nanogels were synthesized according the standard procedure outlined in Figure 1 using 1,2-ethylenediamine as a cross-linker. The *cl*PEO(125)-*b*-PMA(180) nanogels (targeted degree of cross-linking was 20%) with the net negative charge (zeta-potential, ζ =-25-30 mV), diameters of 130-140 nm and relatively low polydispersity indices (0.13-0.15) were prepared. The size and net negative charge of *cl*PEO(125)-*b*-PMA(180) nanogels increased with increasing pH: nanogels shown an increase in the diameters from 130 up to 170 nm when pH of the solution was adjusted from 6 to 9. However, the overall swelling behavior of *cl*PEO(125)-*b*-PMA(180) nanogels was less pronounced compare to *cl*PEO(170)-*b*-PMA(180) nanogels which might be a result of higher degree of cross-linking in the core of the nanogels. Indeed, the estimated number of cross-links per chain was slightly higher in *cl*PEO(125)-b-PMA(180) nanogels than in clPEO(170)-b-PMA(180) nanogels (ca. 5.6 vs 5.0). *cl*PEO(125)-b-PMA(180) nanogels remained stable in aqueous dispersions in a wide range of concentrations (up to 1.5 %), exhibiting no aggregation for several months. The spherical morphology of the nanogels was confirmed by AFM imaging. Samples for AFM imaging were prepared by depositing 5 μL of an

aqueous dispersion of nanogels (ca. 0.2 mg/ml) onto positively charged 1-(3-aminopropyl)silatrane mica surface (APS-mica) for 10 minutes followed by surface washing with deionized water and drying under argon atmosphere. Typical image of *cl*PEO(125)-b-PMA(180) nanogel is presented in ***Figure 6***. "Round-shape" particles with a height of ca. 0.8-0.9 nm and average diameter of 10 nm were observed. It is likely that PEO-*b*-PMA spheres expanded in solutions collapsed on the mica surface upon drying and were visualized by AFM as flattened circular images. The high diameter versus height aspect ratio was in agreement with the expected flexible, shape-adaptable character of these nanostructures imparted by the PMA core "soft" material. These nanogels can be also freeze-dried and reconstituted in aqueous dispersion practically without change in their initial size.

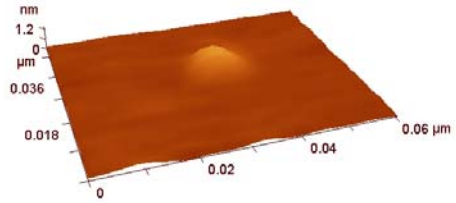

Figure 6. Tapping-mode AFM image of clPEO(125)-*b*-PMA(180) nanogel in air

Task 3 -- Select the antibody to a tumor epitope

Milligram amounts of CC49 IgG, dimer and tetramer have been obtained. The hexahistidine tagged dimeric and tetrameric scFvs were produced in *Pichia pastoris* and purified by affinity chromatography using Ni-NTA columns. The dimer and tetramer were separated by gel filtration chromatography on sephadex G-200 column. The purified proteins were found to be immunoreactive against TAG-72 as determined by solid phase ELISA. The proteins were radioiodinated with ^{125}I by Iodogen method and the unincorporated radioactivity was removed using desalting column. Following radiolabeling and desalting, >99% of the radioactivity was associated with the protein fractions as determined by ITLC. The SDS-PAGE (***Figure 7)*** and HPLC (***Figure 8***) analyses of the radiolabeled proteins indicated no apparent degradation or aggregation. The immunoreactivity of radiolabeled antibodies was determined by solid phase radioimmunoassay using TAG-72 coated beads for specific binding and BSA coated beads for non-specific binding. The specific reactivities of IgG, tetramer and dimer were 95%. 87%

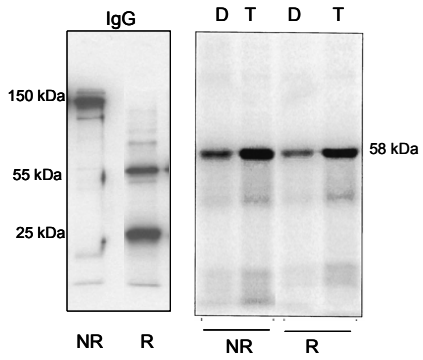

Figure 7. Autoradiography of SDS-PAGE gel of intact CC49 IgG, dimer (D) and tetramer (T) under non-reducing (NR) or reducing (R) conditions.

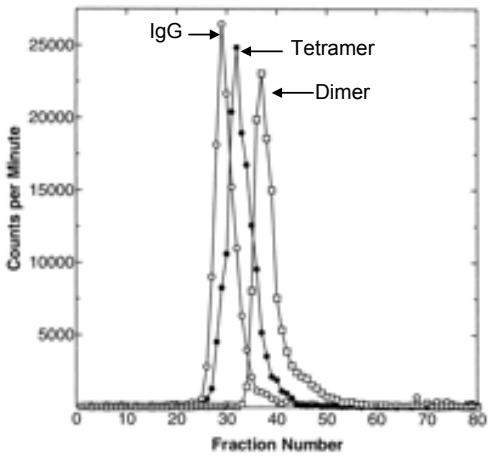

Figure 8. HPLC analysis CC49 IgG, tetramer and dimer following radioiodination with ^{125}I. There is no evidence of degradation following radiolabeling.

and 72%, respectively, while the non specific reactivity was <5% for all the proteins. These reagents would be further utilized for the synthesis of TAG-72-targeted immunodiagnostics applications.

Task 4 -- Develop procedure and synthesize reagents for conjugation of antibody to nanogel

Specific ligands (proteins and peptides) can be coupled to the surface of the nanogels via distal ends of PEO chains. A method of activation of OH-groups with nitrophenyl chloroformate to produce the nitrophenylcarbonate activated polymer is suitable for single-step binding of the variety of amino-containing ligands. Since nitrophenyl carbonates are readily hydrolyzed in the aqueous media, the PEO-activation reactions need to be performed in the organic media. However, lyophilized *cl*PEO(125)-b-PMA(180) nanogels were not soluble in suitable organic solvents such as acetonitrile, THF, ethyl alcohol, dimethylformamide, methyl-2 pyrrolidone. The protonation of carboxylate groups in the cores of nanogels using formic acid/hexane mixture resulted in the formation of white solid that was also not soluble in organic media. Further, the cores of the nanogels were hydorophobized using triethylamine or strong and efficient base, 1,8-diazabicyclo-(5.4.0)-undec-7-ene (DBU). Neither of these core modifications allowed us to dissolve *cl*PEO(125)-b-PMA(180) nanogels in the organic solvents. Therefore, the reactions of activation of end hydroxyl groups of PEO chains in aqueous media were explored. The stable intermediate was prepared by reacting *cl*PEO(125)-b-PMA(180) nanogels with divinyl sulfone (1,1'-sulfonylbisethane, DVS) under controlled pH. DVS was dissolved in THF to allow a better mixing with aqueous dispersions of nanogels. The pH of the dispersion of *cl*PEO(125)-b-PMA(180) nanogels (5 ml) with the final concentration of 12 mM on the base of carboxylic groups was adjusted to 9.6 and 10 uL of DVS (ca. 3 eq. excess in respect to the content of OH-groups) were added upon vigorous mixing followed by the stirring at room temperature. The reaction was quenched after 2 hours by adjusting pH to 6.5. This leaves any unreacted vinyl groups attached to the distal OH-groups of PEO chains in the corona of the nanogels creating an “activated nanogels”. The unreacted DVS and hydrolysis products

were removed by exhaustive dialysis against water. The sizes of *cl*PEO(125)-b-PMA(180)-DVS nanogels were practically the same after the activation step. The product of this reaction is a stable, reactive intermediate that was freeze-dried and further used to conjugate to antibody.

Task 5 -- Conjugate antibody to a nanogel surface

The nanogels were activated using reaction of distal hydroxyl groups of *cl*PEO(125)-b-PMA(180) nanogels with divinyl sulfone as described in task 4. Bovine serum albumin (BSA, M.w. 66.4 kDa) was used as a model protein to validate the conjugation strategy. *cl*PEO(125)-b-PMA(180) nanogels with targeted degree of cross-linking of 100% were used in conjugation reaction. Excess of BSA solution was mixed with the dispersion of *cl*PEO(125)-b-PMA(180)-DV nanogels in carbonate buffer (10 mM, pH 9.6) and reaction mixture was stirred overnight at 4^{o}C followed by dialysis against phosphate buffer (10 mM, pH 7.4). The unbound BSA was further removed by GPC on Sepharose CL-6B column. The extent of conjugation of BSA to the nanogels was monitored SDS-PAGE gel electrophoresis (***Figure 9***). The electrophoresis was conducted under reducing conditions on 10% acrylamide gels with 5 mM Tris, 50 mM Glycine, pH 8.3 running buffer at 80 V for 2 hours in a Bio-Rad Mini-Protein Gel Electrophoresis Cell. 20 μL of each sample was loaded into wells. Unmodified BSA solutions in phosphate buffer and free nanogels were used as controls. The protein bands were visualized by staining in 0.25% with Coomassie blue R-250 in 10% methanol/10% acetic acid. As it seen on gel electrophoresis pattern presented in ***Figure 9*** in the case of BSA-conjugated nanogel there is a portion of protein that is retarded on the start of the gel. In contrast, no band retardation was observed in the lanes corresponding to free BSA or nanogels. This suggested that conjugates formed were enabling to enter the gel. Surprisingly intensive very broad bands were detected for free and BSA-modified nanogels. It might be indicative of existence of some impurities in the initial nanogels or diblock copolymers and this required further detailed investigation.

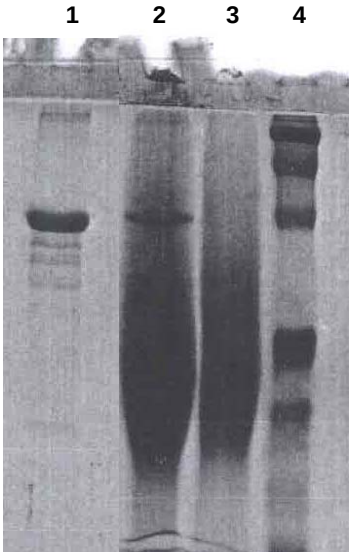

Figure 9. SDS-PAGE gel of (1) free BSA; (2) BSA-conjugated nanogel; (3) free nanogel; and (4) protein ladder under reducing conditions

Task 9 -- Incorporate MR probe in nanogels

Nanogels synthesized as described in Task 2 were modified by introducing a chelating group and the MR probe, Gd(III) were loaded in the modified nanogel. Several synthetic procedures were used to introduce a chelating agent, diethylenetriaminepentaacetic acid (DTPA). First, primary amino groups were introduced into the core of the nanogels via modification of the carboxylic groups of polyion chains with N-Boc-ethylenediamine (ED-Boc) in the presence of EDC hydrochloride (***Figure 10***). The number of the bound Boc units was controlled by the molar ratios of amine functional groups to carboxyl groups in the nanogels. The standard procedure used for the incorporation of Gd(III) into the nanogels is described below.

Introduction of primary amino groups to nanogels. Nanogels (*cl*PEO(170)-*b*-PMA(180))were dissolved in water (concentration of COOH-groups was 1-2x10^{-4} base-mole/L) and freshly prepared aqueous solution of EDC (1.5 eq) was added followed by stirring of the reaction mixture for 10 minutes. N-Boc-ethylenediamine (ED-Boc, 1.2 eq) was dissolved in EtOH (0.2-0.4mL) and mixed with the solution of activated nanogels, pH was adjust to 8. The mixture was stirred at room temperature overnight. Then, the reaction solution was dialyzed first, against 0.5% aqueous ammonia, and then against distilled water. According to ^{1}H NMR analysis the number of N-Boc-EDs bound to one PEO-*b*-PMA chain was calculated to be ca. 30 units. The number of Boc units was found from peak intensity ratio between the methylene protons of the PEO block (3.7 ppm) and the methyl protons of the Boc units (1.4 ppm). The particle size of the *cl*POMA-ED-Boc nanogels was increased from 90-100 nm to 110-120 nm compare to initial *cl*PEO(170)-*b*-PMA(180) nanogels .

Deprotection of primary amino groups. Deprotection of the Boc units was carried out using trifluoroacetic acid. clPOMA-ED-Boc nanogels were dissolved in 3 ml TFA in an iced bath and the mixture was stirred for 1.5 h. Then the TFA was evaporated and 3 ml of water was added followed by dialysis against bi-distilled water. This deprotection reaction proceeded completely, as confirmed by the disappearance of a methyl peak attributed to the Boc units (1.4 ppm) in the ^{1}H NMR spectra. The size of nanogels with additional primary amino groups (cl-POMA-ED) was monitored by DLS and was found to be 140-180 nm.

Conjugation of DTPA to the nanogels. Diethylenetriaminepentaacetic acid bisanhydride (DTPA-ba, 4 eq) was added to the solution of cl-POMA-ED micelles (1 eq) and stirred for 2 h at pH 4

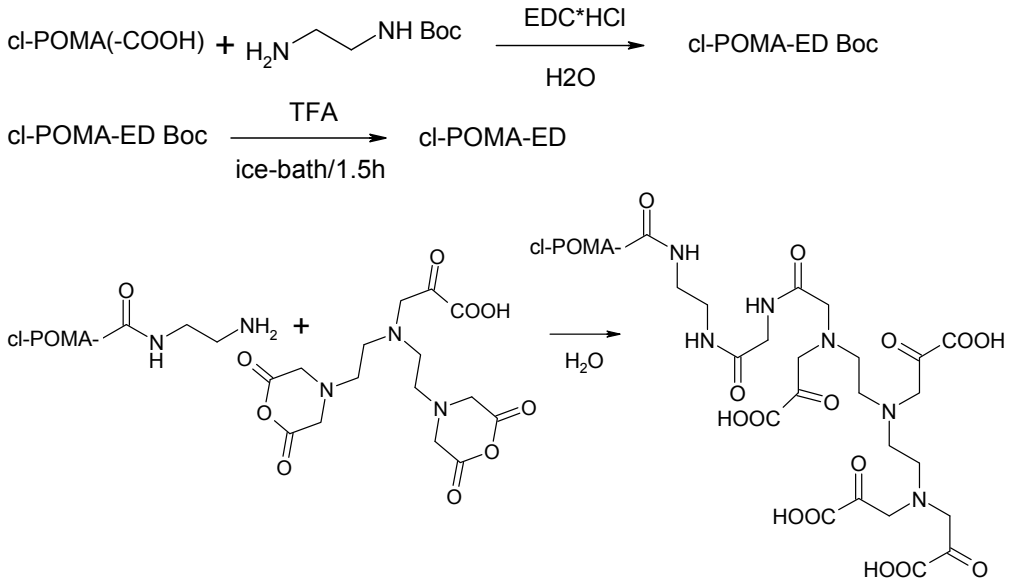

Figure 10. Scheme for the synthesis of PEO-*b*-PMA nanogels modified with chelating agent, DTPA. (PEO-*b*-PMA copolymer is abbreviated as cl-POMA).

followed by overnight stirring of the reaction mixture at pH 6-7 at room temperature. Then, the reaction mixture was dialyzed first, against 0.5% aqueous ammonia, and then against distilled water. The composition of obtained conjugate was determined using ^{1}H NMR. The number of DTPA units per one PEO-*b*-PMA copolymer chain was calculated according to the methylene protons of the PEO block (3.7 ppm) and to the methylene protons of DTPA (3.9 ppm). The number of DTPA units was calculated to be ca. 20-30 units per chain.

Chelating of Gd(III) ions to the nanogels. An aqueous solution of $GdCl_3$ (50 mM) was slowly added to the aqueous dispersions of DTPA-modified nanogels (clPOMA-ED-DTPA) at pH 9.0. After a stirring, an excess of EDTA was added followed by dialysis against 0.5% aqueous ammonia and then against distilled water to remove Gd(III) ions nonspecifically bound to the free carboxylic groups in the cores of nanogels. The amount Gd(III) bound to nanogels was calculated using Inductively Coupled Plasma spectrometry (ICP-MS). The T_1 longitudinal relaxation time of Gd-loaded nanogels was estimated from ^{1}H NMR spectra acquired using a Varian INOVA 500MHz spectrometer and relaxivity (R_1) was calculated. In addition, relaxivity of the synthesized Gd-loaded nanogels was determined on 7 T Bruker Advance system.

Specifically, DTPA-modified sample of PEO(170)-*b*-PMA(180) nanogels containing ca. 22 DTPA units per chain was loaded with Gd(III) ions. The amount of Gd(III) incorporated into nanogels was calculated to be 116 μmol Gd per mg of polymer. The topology of Gd-loaded nanogels was further studied by AFM imaging. The loading of Gd(III) into the nanogels did not result in the change of the spherical morphology as was confirmed by AFM imaging. ***Figure 11***

demonstrates typical images of images of DTPA-modified and Gd-loaded nanogels. Gd binding to the DTPA-nanogels resulted in the profound decrease of their size. Indeed, the dimensions of DTPA-modified nanogels determined by analysis of AFM images using Femtoscan software (Advanced Technologies Center, Moscow, Russia) were 25.16 ± 0.49 nm (height) and 73.89 ± 2.26 nm (diameter). The left image in ***Figure 11*** shows Gd-loaded nanogels as almost perfect round particles with a number-averaged height of 11.32 ± 0.21 nm and diameter of 30.04 ± 0.43 nm.

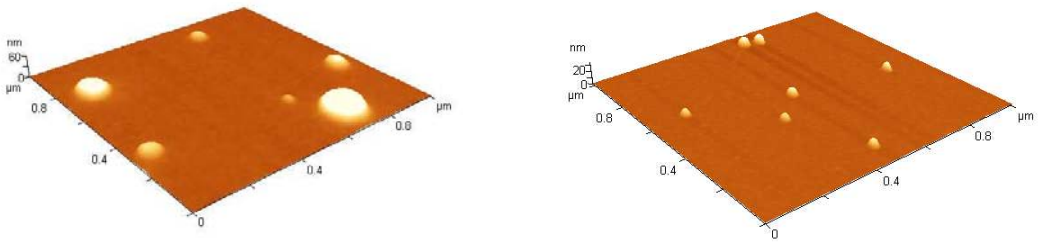

Figure 11. Tapping-mode AFM images of clPEO(170)-*b*-PMA(180) nanogels modified with DTPA (left) and Gd-DTPA-modified nanogels (right) in air. Scan size is 1 μm.

However, these Gd-loaded nanogels had a very low relaxivity (R_1 = 0.84 $mM^{-1}s^{-1}$) compare to small-molecule Gd-DTPA chelate (R_1 value of 3.8 $mM^{-1}s^{-1}$). The process of T_1 shortening requires the direct interaction between protons and the magnetic parts of the contrast agent: hydrogen nuclei of water must be close to the magnetic particles to obtain relaxation enhancement. It is likely that in nanogels with the ionic cores that modified with DTPA-groups in high extent, Gd-ions might be buried within the collapsed partially hydrophobized cores (see Figure 11). Water molecules will have restricted access to the inner Gd-ions of the nanogels and, as a result, ionic relaxivity of such constructs is decreased. Furthermore, this batch of the Gd-DTPA-containing nanogls also exhibited a low stability at physiological conditions. Indeed, progressive aggregation and precipitation of Gd-loaded nanogels was observed in PBS buffer (pH 7.4, 0.14 M NaCl). This is reinforcing our conclusion that high degree of modification of nanogels with Gd-DTPA moieties might result in lost of the stability of nanogels and suppression of ionic relaxivity.

To overcome this problem, the nanogels with a lower degree of modification with DTPA ligands were prepared. Due to the side reactions during the cross-linking of the template PEO(170)-*b*-PMA(180)/Ca^{2+} micelles, the synthesized nanogels always possess free primary

amino groups. The number of these amino groups can be additionally increased by changing the molar ratio between EDC and cross-linked used in the reaction of cross-linking. The modification of these functional groups was further explored upon direct reacting with DTPA bisanhydride. The nanogels with targeted degree of cross-linking of 60% were synthesized using this chemical route and then purified, characterized, and loaded with Gd-ions as described above. The physicochemical characteristics of two samples of Gd-modified *cl*PEO(170)-*b*-PMA(180) nanogels prepared using the same complex template but various amount of DTPA bisanhydride are presented in **Table 4**. In contrast to the previously described nanogels with high content of Gd, both these samples of Gd-loaded nanogels were stable in PBS buffer for at least a week and had a higher relaxivity (5.2 $mM^{-1}s^{-1}$) than Gd-DTPA analog.

The chemical route involving the modification of the PEO-chains in the corona of the nanogels with DTPA moieties was also explored. Hydroxyl groups on the distal ends of PEO chains in the corona of *cl*PEO(125)-*b*-PMA(180) nanogels were first activated with divinyl sulfone (3 eq. excess) and then reacted with an excess of ethylenediamine. It should be noted that the cores of the *cl*PEO(125)-*b*-PMA(180) nanogels used in these reactions were intentionally loaded with Ca^{2+} ions to make the cores more rigid and prevent the reactions between DVS and free amino groups that present in the cores.

Table 4. Physicichemical characteristics of Gd-loaded *cl*PEO(170)-*b*-PMA(180) nanogels

Sample	D_{eff}, nm	PDI	Gd content, mM	R_1, $mM^{-1}s^{-1}$
*cl*PEO(170)-*b*-PMA(180)/Ca^{2+} (template)	123	0.11		
*cl*PEO(170)-*b*-PMA(180)-DTPA(1eq.)	92	0.12		
*cl*PEO(170)-*b*-PMA(180)-DTPA(4eq.)	87	0.15		
*cl*PEO(170)-*b*-PMA(180)-DTPA(1eq.)/Gd	121	0.06	0.0094	5.2
*cl*PEO(170)-*b*-PMA(180)-DTPA(4eq.)/Gd	146	0.22	0.0226	5.2

Nanogels with the amino-functionalized diatal ends of PEO chains in the coronas were obtained in this step. Further DTPA-chelates were conjugated to the amino-modified via reaction with DTPA bisanhydride. The resulting DTPA-modified nanogels had averaged diameters of ca. 140

nm (polydispersity index was 0.11) and a net negative charge (ζ=-21.5 ± 3.7 mV at pH 5.3). Loading of Gd(III) ions into the nanogesl was carried out at pH 9.5. Excess of EDTA was added to remove all nonspecifically bounded Gd-ions. The Gd-loaded nanogel particles were 174 nm in diameter (polydispersity index 0.08) and had a zeta-potential of -22 mV at pH 9.3. These nanogels exhibited good dispersion stability; practically no change in the size of the nanogels was detected during the incubation of nanogels in PBS buffer at 37^{o}C for one week. The concentration of Gd in the resulting dispersion of nanogels was determined to be quite low, 0.001 mM (ICP-MS), compare to the previously synthesized *cl*PEO(170)-*b*-PMA(180)-DTPA-Gd nanogels. However, the preliminary data on relaxivity of this sample revealed a very high value of ca. 108 $mM^{-1}s^{-1}$. The detailed characterization of these nanogel samples is currently ongoing in our laboratories.

Task 11 -- Incorporate luminescence probe (quantum dots) in nanogels

Near-infrared fluorescent probes (NIRF) were used for nanogel labeling. Nanogels with the free amino groups in the core were conjugated with succinimydil ester of Alexa 680 carboxylic acid (Invitrogen) using a protocol provided by manufacturer. The nanogels were purified from non-reacted dye by gel filtration on Sephadex G-25 column in phospahe buffer following the dialysis against distilled water. An average degree of labeling of NIRF-nanogels was 1.8 nmol of NIRF per mg of polymer as was determined by measuring absorbance (184,000 $M^{-1}cm^{-1}$ at 679 nm) using SpectraMax M5 microplate reader. The labeled nanogels were freeze-dried and than readily redispersed in buffered saline. The Alexa 680-labeled nanogels retained their stability in PBS dispersion at 37^{o}C for at least one week.

Task 12 -- Demonstrate tumor detection in an animal model using luminescence

The in vivo migration and localization of NIRF-labeled nanogels were evaluated in athymic nude mice (NC*r-nu/nu*) obtained from NCI (Bethesda, MD) using optical imaging. All in vivo experiments were performed in accordance to animal protocol approved by UNMC IACUC and USAMRMC ACURO. The objective of these experiments was to determine an amount of the probe needed for detection of the tumor. Mice bearing subcuteniosly implanted

tumors (model **I**) were used in these experiments. A subcutaneous solid tumor was established by s.c. injection of human colon carcinoma LS-174T cells ($5x10^6$ in 100 μl of culture medium) onto the back between scapulae in mice to induce tumor growth. Tumors were allowed to progress until they reach a size of about 300 mm^3.

In vivo optical imaging was performed on anesthetized mice with an IVIS 200 small animal imaging system (Xenogen). Identical illumination settings (lamp voltage, filters, f/stop, field of views, binning) were used for acquiring all images. Images were acquired and analyzed using Living Image software (Xenogen). Prior the imaging mice were kept on a special purified diet to reduce the interfering fluorescence signals in the stomach and intestine that are induced by the standard animal food. Each animal was anesthetized in the induction chamber using isoflurane. Immediately after the animal is in a light plane of anesthesia, it will be placed on a manifold nose cone in the IVIS 200 to maintain the anesthesia. Images acquired for the same animals before injection of labeled nanogels were used as controls.

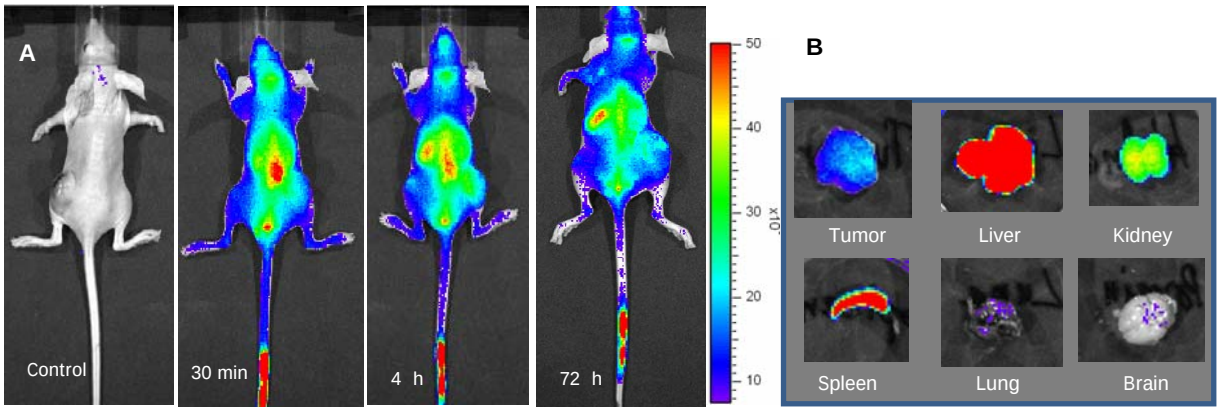

Figure 12. (A) Whole body optical imaging in mice bearing subcutaneous xenografts produced from LS-174T cells after i.v. administration of Alexa 680-labeled nanogels (0.85 nmol NIRF probe per animal). (B) Images of the organs and tumor 72 hours post injection.

Initially, imaging will be performed after i.v. administration of solutions with various concentrations of Alexa 680-labeled nanogels (0.3, 0.6, and 0.85 nmol NIRF/150 ul/animal) prepared in sterile saline. The in vivo fluorescence of Alexa 680-labeled nanogels was tracked over a 72-hour period. After imaging, the tumor, liver, kidney, spleen, and brain were removed and imaged using the same instrument settings. The acquired images are presented in ***Figure 12***. Accumulation of Alexa 680-labeled nanogels in the tumor was observed already 30 min post i.v. injection. Fluorescence signal corresponding to labeled nanogels was also detected in the tumor of the mouse in 72 h after dozing with nanogel probe. However, the liver and spleen showed the most prominent fluorescent signal. Similar results were obtained upon injection of 0.6 nmol

(equivalent of Alexa 680) of Alexa 680-labeled nanogels per animal. This dose is corresponding to ca. 300 μg of the injected polymeric carrier. No reliable fluorescent signal was observed in the tumor upon injection of 0.3 nmol of Alexa 680-labeled nanogels. Overall, these data suggest that NIR-emissive nanogel probes are suitable for the detecting in vivo tumors at relatively low concentration of the probe (0.6 nmol NIRF probe per animal).

KEY RESEARCH ACCOMPLISHMENTS

- Representative panel of nanogels was synthesized using diblock copolymers of different structure and compositions.
- The chemical structure of the block copolymer is a key parameter determining the formation of templates for the nanofabrication of nanogels.
- Metal ions with higher binding affinity to carboxylic groups are required for the formation of polyion/metal complexes using copolymers containing poly(acrylic acid) segments or copolymers with high contents of PEO units. The diblock copolymers with approximately equal lengths of both nonionic and ionic segments might be preferable for the formation of complex templates.
- The physicochemical characteristics of the nanogels (dimensions, swelling behavior) can be tuned by changing the cross-linking density of the cores of the nanogels or by using cross-linkers with different chemical structures. The incorporation of more hydrophobic cross-linkers into the core of the nanogels resulted in the formation of nanogels with smaller sizes and with higher density of cross-links.
- The antibodies to TAG72 specific to colon cancer cells were generated, purified and characterized.
- Procedure for incorporation of reactive groups at the nanogel surface in aqueous media was developed.
- Paramagnetic Gd(III) ions were incorporated into the nanogels via stable DTPA-chelates. Ionic relaxivity (R_1) of Gd-loaded nanogels thus prepared was tested at magnetic field strength of 7 Tesla utilizing a progressive saturation pulse sequence. First generation of Gd-loaded nanogels had a higher relaxivity (5.2 $mM^{-1}s^{-1}$) than the small-molecule Gd-DTPA chelate (3.8 $s^{-1}mM^{-1}$).
- Near-infrared fluorescent probe were introduced into the cores of nanogels.
- “Proof-of-principle” optical imaging studies demonstrated that NIR-emissive nanogel probes are suitable for the detecting in vivo tumors at relatively low concentration of the probe (0.6 nmol NIRF probe per animal).

REPORTABLE OUTCOMES

- Interdisciplinary research team of scientist with an extensive expertise in the fields of material science, pharmacy, cancer research, and medicine was assembled.
- State-of-art equipment for the characterization of nanomaterials was acquired was acquired.
- A platform nanotechnology for the delivery of imaging and diagnostic agents based on hydrophilic polymer nanogesl of core-shell morphology was established.
- Key structural parameters of block copolymers governing the physicochemical properties of the nanogels were identified.
- Anti-TAG72 antibodies (MAb CC49) were generated, purified and characterized.
- The nanogels loaded with MR probe, Gd(III), or optical near-infrared fluorescent probe were developed.
- Animal protocol was established and approved by UNMC IACUC and USAMRMC ACURO.
- “Proof-of-principle” optical imaging studies demonstrated that NIR-emissive nanogel probes are suitable for the detecting in vivo tumors.

CONCUSION

- Representative panel of nanogels was synthesized using diblock copolymers of different structure and compositions. The chemical structure of the block copolymer is a key parameter determining the formation of templates for the nanofabrication of nanogels. The structure of cross-linker and number of cross-links dictate the composition and properties of the nanogel core. The number of cross-links in the core directly controls the swelling behavior of the core of nanogel and thus the size of the nanogels. This, in turn, affects loading efficiency of the nanogels, their stability at physiological conditions. The presence of the highly charged ionic cores is preventing the dissolution of the nanogels in common organic solvents. Therefore, the development of robust procedures for incorporation of reactive groups at the nanogel surface in the aqueous media is necessary. Currently, activation of distal hydroxyl groups of PEO chains forming the shells of nanogels was achieved using divinyl sulfone. Alternatively, antibodies can be attached to nanogel core through a poly(ethylene oxide) linkers. Heterobifunctional PEO with maleimide- and amine-modified terminal groups will be used to react with sulfhydryl group of anibidies to form stable thioether bonds. The amino-functionalized PEO-antibody constructs will be further covalently attached to the acid residues within the core of nanogels using EDC –mediated coupling reaction. Gd(III) ions were incorporated into the nanogels via stable DTPA-chelates. It was demonstrated that the dispersion stability and relaxivity of Gd-loaded nanogels are strongly affected by the extent of DTPA-modification of nanogels. This parameter will be optimized in our future studies. Near-infrared fluorescent probe were introduced into the cores of nanogels. “Proof-of –principle” optical imaging studies demonstrated that NIR-emissive nanogel probes are suitable for the detecting in vivo tumors at relatively low concentration of the probe (0.6 nmol NIRF probe per animal).